Nuclear Magnetic Resonance Study of the Schiff Base in Bacteriorhodopsin: Counterion Effects on the ^{15}N Shift Anisotropy†

H. J. M. de Groot,‡,§,‖ G. S. Harbison,⊥ J. Herzfeld,§ and R. G. Griffin*,‡

Francis Bitter National Magnet Laboratory, Massachusetts Institute of Technology, Cambridge, Massachusetts 02139, Department of Chemistry, Brandeis University, Waltham, Massachusetts 02254, and Department of Chemistry, State University of New York, Stony Brook, New York 11794-3400

Received August 30, 1988; Revised Manuscript Received October 21, 1988

ABSTRACT: High-resolution, solid-state ^{15}N NMR has been used to study the chemical shift anisotropies of the Schiff bases in bacteriorhodopsin (bR) and in an extensive series of model compounds. Using slow-spinning techniques, we are able to obtain sufficient rotational sideband intensity to determine the full ^{15}N chemical shift anisotropy for the Schiff base nitrogen in bR_{548} and bR_{568}. Comparisons are made between *all-trans*-bR_{568} and *N-all-trans*-retinylidene butylimine salts with halide, phenolate, and carboxylate counterions. It is argued that for the model compounds the variation in ^{15}N chemical shift reflects the variation in (hydrogen) bond strength with the various counterions. The results suggest that carboxylates and tyrosinates may form hydrogen bonds of comparable strength in a hydrophobic environment. Thus, the hydrogen bonding strength of a counterion depends on factors that are not completely reflected in the solution pK_a of its conjugate acid. For the model compounds, the two most downfield principal values of the ^{15}N chemical shift tensor, σ_{22} and σ_{33}, vary dramatically with different counterions, whereas σ_{11} remains essentially unaffected. In addition, there exists a linear correlation between σ_{22} and σ_{33}, which suggests that a single mechanism is responsible for the variation in chemical shifts present in all three classes of model compounds. The data for bR_{568} follow this trend, but the isotropic shift is 11 ppm further upfield than any of the model compounds. This extreme value suggests an unusually weak hydrogen bond in the protein.

Despite intensive study, bioenergetic processes in membrane proteins are still not well understood. One of the most thoroughly investigated systems is undoubtedly bacteriorhodopsin (bR),[1] the purple light-harvesting membrane protein of *Halobacterium halobium* which converts light energy into a proton gradient across the bacterial membrane [for a review, see, e.g., Stoeckenius and Bogomolni (1982)]. The bR polypeptide chain (Khorana et al., 1979; Ovchinnikov et al., 1979) is folded into seven transmembrane segments (Henderson & Unwin, 1975) and contains a retinal chromophore that forms a Schiff base linkage with the ϵ-nitrogen of the lysine-216 residue (Khorana et al., 1979; Rothschild et al., 1982).

It is well established that the Schiff base in bR is protonated. Evidence for this has been obtained by a variety of experimental approaches: laser Raman spectroscopy (Lewis et al., 1974; Aton et al., 1977; Ehrenberg et al., 1980; Doukas et al., 1981; Hildebrandt & Stockburger, 1984), FTIR (Bagley et al., 1982; Rothschild & Marrero, 1982), and high-resolution solid-state NMR (Harbison et al., 1983). Protonation of the Schiff base places a positive charge on the chromophore, and the distribution of this positive charge is directly related to the excitation energy in the optical spectrum (Kropf & Hubbard, 1958)—greater delocalization leads to an increased red shift in the absorption maximum. This effect is commonly referred to as the *opsin shift* and is defined as the difference between the frequency of the maximum of absorption of fully light-adapted bR, which has an all-trans chromophore, and that of the protonated *all-trans*-retinal Schiff base in solution. In bR, this amounts to $\sim$5100 cm^{-1} (λ_{max} 440 $\rightarrow$ 570 nm).

Previous FTIR (Rothschild & Marrero, 1982; Bagley et al., 1982), laser Raman (Smith et al., 1987; Hildebrandt & Stockburger, 1984), and NMR studies (Harbison et al., 1983, 1985a,b), together with chemical analogue experiments (Nakanishi et al., 1980; Lugtenburg et al., 1986; Spudich et al., 1986) and theoretical calculations (Honig et al., 1976), have contributed to our present understanding of the electronic properties of the chromophore in bR. It appears that several mechanisms contribute to the opsin shift, the three most important being the configuration of the 6–7 (6-s) single bond, which influences the extension of the π-electron system into the the β-ionone ring, the strength of the hydrogen bond at the Schiff base, and electrostatic interactions with other nearby protein charges [see, e.g., Lugtenburg et al. (1986) and references cited therein]. The importance of the hydrogen bonding of the Schiff base may also be appreciated by comparing the $pK_a > 12$ of the Schiff base in bR (Ehrenberg et al., 1980; Doukas et al., 1981; Druckmann et al., 1982) with the $pK_a \simeq 7$ typically observed for protonated Schiff base model compounds (Favrot et al., 1978).

Early theoretical considerations suggested that a change in counterion–nitrogen distance from 3 Å to infinity (i.e., breaking the hydrogen bond) could in principle give rise to a very strong N–H bond and a shift in the absorption maxi-

† This research was supported by the National Institutes of Health (GM36810, GM23289, and RR00995). H.J.M.d.G. is a recipient of a fellowship (S81-346) from the Netherlands Organization for the Advancement of Pure Research (ZWO) and was also awarded a research career development fellowship (Academie-onderzoeker) from the Royal Netherlands Academy of Sciences (KNAW).

* To whom correspondence should be addressed.

‡ Massachusetts Institute of Technology.

§ Brandeis University.

‖ On leave from the Gorlaeus Laboratories, Rijksuniversiteit te Leiden, The Netherlands.

⊥ State University of New York at Stony Brook.

[1] Abbreviations: bR, bacteriorhodopsin; CP, cross-polarization; FWHM, full width at half-maximum; MAS, magic angle spinning; PSB, protonated Schiff base.

0006-2960/89/0428-3346$01.50/0

mum from 440 nm (close to the observed λ_{max} for protonated Schiff bases in solution) to 600 nm (well above the absorption maximum in a fully light-adapted purple membrane, λ_{max} = 568 nm). For Schiff base model compounds, it has been demonstrated that substitution of a large for a small counterion (which is thought to be equivalent to increasing the counterion distance) does indeed shift λ_{max} to the red in aprotic solvents. However, the observed shifts in these model systems are rather small (Blatz & Mohler, 1975; Sheves & Nakanishi, 1983; Childs et al., 1987). Since decreasing the strength of the counterion interaction also tends to decrease the C=N stretch frequency, the experimental observation that the C=N stretch in bR is considerably lower (1640 cm^{-1}) (Ehrenberg et al., 1980) than in comparable protonated retinal Schiff bases (1646–1658 cm^{-1}) (Heyde et al., 1971; Blatz & Mohler, 1975; Mathies et al., 1977; Smith et al., 1985; Sandorfy et al., 1987) provides additional evidence for an unusually weak hydrogen bond in bR (Rodman-Gilson et al., 1988).

The unusual character of the N–H bond in bR has motivated us to perform a detailed investigation of the chemical shifts associated with the Schiff base nitrogen using high-resolution MAS NMR techniques. Solid-state MAS NMR offers important advantages over the more conventional solution NMR methods in that all three principal values of the chemical shift tensor can be measured instead of just the average value (the isotropic shift, σ_i). Observed variations in the shift tensor elements of model compounds can be correlated with different types of interactions and used empirically to provide structural interpretations of the shift tensor elements of more complex systems. This strategy has proved effective in our ^{13}C NMR studies of the bR chromophore (Harbison et al., 1985a,b).

Our earlier ^{15}N NMR studies of the Schiff base in bR (Harbison et al., 1983) were performed by growing *Halobacterium halobium* on a defined medium containing [ϵ-^{15}N]lysine, to specifically label the lysine side chains. It was possible to observe the ^{15}N resonances of the Schiff base of the all-trans (bR_{568}) and 13-cis (bR_{548}) isomers in dark-adapted bR, and the isotropic shifts of these resonances (143.5 and 150.6 ppm) were much closer to those of protonated (154–175 ppm) than to unprotonated Schiff bases (~300 ppm), unambiguously establishing the protonation state of the nitrogen. In addition, it was shown that over the series of halide salts of *N*-retinylidene butylimine (Cl^-, Br^-, I^-), there existed a pronounced variation in isotropic chemical shifts, such that iodide (154.4 ppm) was about 17 ppm upfield of chloride (171.7 ppm) and much closer to bR (143.5 ppm, 150.6 ppm). Considering that the larger and more highly polarizable iodide ion forms a much weaker hydrogen bond than the small "hard" chloride, it was suggested that the ^{15}N chemical shift in bR reflects the strength of the interaction between the Schiff base proton and charges in the surrounding protein environment. In order to better understand this phenomenon, we have now obtained results on an extended series of Schiff base salts with monovalent counterions.

In the earlier report, chemical shift anisotropy data were presented for PSB model compounds. However, for bR it was not possible to record spectra of the quality required to determine the tensor elements. With recent improvements in instrumentation, primarily low-temperature spectroscopy and accurate control of the spinning speed, we are now able to record high-quality ^{15}N spectra of bR. At low temperatures, the Schiff base proton exchange (Harbison et al., 1988) is quenched, and we obtained the three principal values of the ^{15}N chemical shift tensor in bR, which can be compared with those in the model compounds.

Materials and Methods

[ϵ-^{15}N]Lysine bR was prepared by growing *Halobacterium halobium* R_1 on a synthetic medium similar to that used previously by Gochnauer and Kushner (1969) in which [ϵ-^{15}N]lysine was substituted for the unlabeled lysine normally present (Argade et al., 1981). The incorporation was verified by using trace [^{3}H]lysine, and labeling was determined to be at least 95%. The purple membrane was isolated by using the purification procedure of Oesterhelt and Stoeckenius (1974). The equivalent of approximately 100 mg of protein was pelleted tightly in a centrifuge and then packed in an alumina rotor.

all-trans-Retinylidene [^{15}N]butylimine was prepared as described by Harbison et al. (1983). Trifluoroacetic, trichloroacetic, tribromoacetic, dichloroacetic, difluoroacetic, and picric acids were purchased from Aldrich Chemical Co. (Milwaukee, WI). Except for the picric acid, which was kept under vacuum in order to remove possible water contamination, these compounds were used without further purification. 2,6-Dibromo-4-nitrophenol (Linnemann & Stersch, 1867) and 2-chloro-4,6-dinitrophenol (Hodgson & Smith, 1931; Holleman, 1902) were synthesized by published procedures. Chloride- and bromide-protonated Schiff base salts were prepared by treating the ^{15}N Schiff bases in anhydrous diethyl ether at −40 °C with a 5% excess of the requisite acid dissolved in a minimum amount of dry ether. The other salts were obtained by an analogous treatment in hexane. Crystallization at −40 °C either occurred spontaneously or was induced by trituration of the container with a glass rod. The salts were then filtered, and, if necessary, recrystallized from hexane or chloroform/ether. We also tried to prepare solid salts with acids weaker than 2-chloro-4,6-dinitrophenol or dichloroacetic acid. While weaker acids apparently protonate retinal Schiff bases in ether or hexane, attempts to crystallize the products led only to viscous, highly colored oils.

The NMR data were collected with a home-built spectrometer and probes operating at ^{1}H and ^{15}N frequencies of 317 and 32.2 MHz. The ^{15}N and ^{1}H pulse lengths are typically 10 and 3 μs, respectively, and all experiments used the standard CP and MAS techniques with proton decoupling during acquisition (Andrew et al., 1958; Pines et al., 1973; Griffin et al., 1988). Recycle delays were 1–2 s, and mixing times were 1–2 ms. Chemical shifts were referenced to external 5.6 M $^{15}NH_4Cl$ in H_2O.

Originally, the probes were equipped with magic angle spinners of the Andrew–Beams design, and such probes were used for some of the model compound MAS experiments. More recently, these spinners were replaced with an assembly purchased from Doty Scientific, Inc. (Columbia, SC), which utilizes sealed rotors that can contain wet samples. The bR experiments used the latter system, and it should be emphasized that care was taken to ensure that the bR sample was fully hydrated.

An important aspect of the present work is the determination of the chemical shift anisotropy for the bR_{548} and bR_{568} resonances from rotational sideband intensities. An accurate measurement is only possible if the spinning speed ω_r is sufficiently small that at least two sets of sidebands for each species are clearly visible in the MAS spectrum. Furthermore, overlap between sidebands and other peaks in the spectrum is to be avoided. In protonated Schiff bases, the anisotropy $\delta = \sigma_{zz} - (1/3)Tr(\sigma)$ is small (−5 to −4 kHz), and, therefore, the optimum spinning speed to satisfy the above conditions is 1.120 kHz. However, it is difficult to acquire a spectrum

at such low ω_r, because the intensity of the Schiff base nitrogen lines, which are already the weakest lines in the spectrum, will be dispersed over many peaks. In order to maximize the signal-to-noise ratio, and enhance data collection rates, the bR spectra were recorded at temperatures of −75 to −80 °C. In addition, by using a spinning speed controller that was recently constructed in our laboratory (de Groot et al., 1988), we were able to maintain a constant spinning speed (±2 Hz) over the full measurement time. This prevents broadening of the sidebands. With these two instrumental improvements, we were able to obtain a spectrum of sufficient quality in about 2 days.

It was not necessary to observe these precautions in the investigation of the PSB model compound, since a spectrum with sufficient signal-to-noise ratio was obtained in a few minutes. In addition, spectra of static samples of PSB model compounds were investigated. In those cases, acquisition times were typically 15 min. Shielding tensor principal values were obtained from the singularities in the powder spectra, and isotropic chemical shifts were obtained from the MAS spectra.

The procedure followed in recording the bR NMR spectra was as follows. Spectra were recorded successively at high speed (ω_r = 3.000 kHz) and at low speed (ω_r = 1.120 Hz), so that both spectra were obtained under exactly the same experimental conditions. The chemical shift tensor elements were calculated by serial analysis of these two spectra, excluding the signal from the six free lysine residues. The spectrum at high speed contains only very weak sidebands and is therefore largely independent of the chemical shift anisotropy. This spectrum can therefore be used to determine the relative intensities of the contributions from bR_{548}, bR_{568}, and the natural-abundance ^{15}N in the peptide backbone. In addition, the isotropic chemical shift, σ_i, and line width for each component can be measured. These data were then taken as fixed parameter values in the analysis of the second (low speed) spectrum. In addition, the anisotropy parameters for the natural-abundance background, which have been obtained from an independent measurement of the chemical shift tensor of an unlabeled sample, were entered as fixed parameters. In this manner, the number of free parameters for the fit of the second spectrum is greatly reduced, yielding an enhanced accuracy and better convergence. The entire downfield region of the spectrum was fit with seven parameters; four nonlinear parameters for the anisotropy of the bR_{548} and bR_{568} tensors, one linear parameter for the total intensity, and two linear parameters for a first-order background correction. The computer analysis was performed on a MicroVAX-II, using various approaches for the calculation of the MAS spectra (Maricq & Waugh, 1979; Herzfeld & Berger, 1980) and the CERN fitting package MINUIT (CERN, Geneva).

Results

In Figure 1, we show MAS spectra for dark-adapted [ϵ-^{15}N]lysine-labeled bR, at spinning speeds ω_r = 3.000 kHz (Figure 1a) and ω_r = 1.120 Hz (Figure 1b). In Figure 1a, we see the same features that have been reported earlier (Harbison et al., 1983), but with much improved signal-to-noise ratio. Centered around 147 ppm are two small lines from the Schiff base nitrogen, the downfield line of the pair being assigned to bR_{548} and the upfield peak to bR_{568} (Harbison et al., 1983). The intensity ratio between bR_{568} and bR_{548} is approximately 1:1. The lines are fairly broad, FWHM ≃ 3.5 ppm, which is more than twice the width observed for carbons in the remainder of the conjugated system (FWHM ≃ 1.1–1.3 ppm). The broadening appears to be independent of temperature and suggests local disorder around the Schiff base

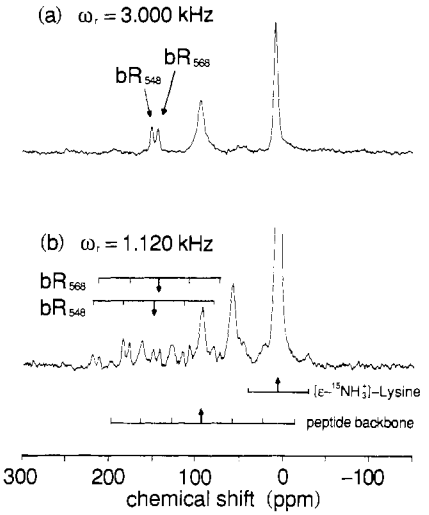

FIGURE 1: Proton-decoupled ^{15}N CP/MAS spectra for [ϵ-^{15}N]lysine purple membrane (bR_{560}) at two different spinning speeds, ω_r = 3.000 kHz (a) and ω_r = 1.120 kHz (b). The centerbands of various components are indicated by arrows. In addition, the sidebands corresponding to each centerband are indicated in (b). The sample temperature for both spectra was between −75 and −80 °C.

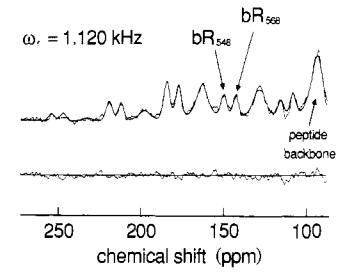

FIGURE 2: Results of the analysis of the downfield region of the spectrum of Figure 1b. The upper part compares the experimental NMR spectrum (thin wavy line) with the theoretical fit (thick line), whereas the lower part gives the residue, i.e., the difference between data and theory.

linkage. The broad envelope at 94.6 ppm is the signal of the natural-abundance ^{15}N in the amide linkages of the peptide backbone. Finally, the sharp intense peak at 8.4 ppm is due to the ϵ-NH_3^+ groups of the lysine residues that are not involved in the Schiff base linkage.

Since the spectrum shown in Figure 1a was taken with a high spinning speed, the majority of the spectral intensity is found in the centerbands. For instance, the first set of sidebands of the amide pattern is barely visible at 0 and 187 ppm. In contrast, in the slow spinning spectrum of Figure 1b, a rich spectrum of centerbands and sidebands is observed for each component.

In Figure 2, the low-speed spectrum is compared with the spectrum calculated by using the input parameters and procedures discussed above. Only the downfield region was included in the fit, to avoid interference with the weak sidebands of the ϵ-lys-NH_3^+ pattern. The results are summarized in Table I. The shift tensor data for halide, phenolate, and carboxylate model compounds are listed in Table II.

Discussion

Examination of the ^{15}N shielding tensor data for the Schiff base model compounds and bR reveals two striking trends. First, while there is clearly a wide range of isotropic chemical shifts, σ_i, the upfield principal value, σ_{11}, is essentially constant within a counterion class and varies relatively little between classes and bR. Therefore, the large differences in isotropic

Table I: ^{15}N Shift Tensor Elements (σ_{11}, σ_{22}, and σ_{33}) and Isotropic Shifts (σ_i) from MAS Experiments for Various Components in bR Spectra[a]

	σ_{11}	σ_{22}	σ_{33}	σ_i
[ϵ-^{15}N]Lys-labeled bR				
bR_{568} (all-trans)	14 (8)	157 (8)	260 (7)	143.5 (0.2)
bR_{548} (13-cis)	13 (8)	178 (8)	260 (7)	150.6 (0.2)
amide backbone	20 (4)	56 (4)	206 (4)	93.6 (0.2)
ϵ-Lys-$^{15}NH_3^+$				8.4 (0.2)

[a] All shifts are given in ppm relative to external 5.6 M $^{15}NH_4Cl$ in H_2O. The errors for the principal values are statistically determined and represent a 95% confidence interval. The errors for σ_i are determined by the accuracy of the calibration and are estimated.

shift are mainly due to variations in σ_{22} and σ_{33}. Second, for the all-trans PSB model compounds *and* bR_{568} (in which the chromophore is also all-trans), there appears to be a strong linear correlation between σ_{22} and σ_{33}, as is illustrated in Figure 3.

With regard to the invariance of the σ_{11} element of the ^{15}N shift tensor, it should be noted that localized changes in shift tensor elements have been observed previously in ^{13}C spectra in several different cases. In carboxyls and carbonyls, it was found that σ_{11} and σ_{33} were virtually invariant to structural changes and the variation in isotropic shift was essentially resident in σ_{22} (Pines et al., 1973). Similarly, deprotonation of substituted phenols to form phenolates changes σ_{22}, while σ_{11} and σ_{33} remain fixed (Smith et al., 1986). In addition, γ effects attributed to steric interactions have been observed to alter only the σ_{11} element in *p*-dimethoxybenzene (Maricq & Waugh, 1979), in polyacetylene (Mehring et al., 1982; Terao et al., 1984), and in retinal (Harbison et al., 1985b). The latter observations contrasted with the *invariance* of σ_{11} in the ^{15}N Schiff base tensors argues against any significant role for steric perturbations in the spectroscopy of the Schiff base nitrogen.

The existence of the striking monotonic relationship between σ_{22} and σ_{33} is surprising within a single class of counterions, and even more so among the three different classes of counterions and bR_{568}. This suggests that the chemical shifts of the Schiff base nitrogen are determined by a single dominant factor. We shall argue that this factor is most likely the strength of the nitrogen–counterion hydrogen bond, and that the data for bR therefore require an exceedingly weak hydrogen bond in the protein.

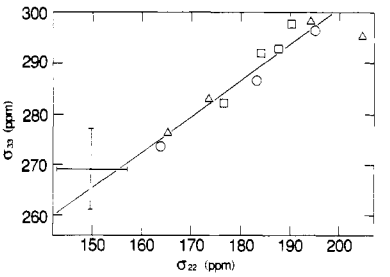

FIGURE 3: Principal values of the chemical shift tensor σ_{33} versus σ_{22} for the all-trans PSB model compounds (cf. Table II) and the all-trans form of the protein bR_{568} (cf. Table I). The solid line was plotted according to a linear regression analysis of the model compound data, excluding the data point for the trifluoroacetic acid salt. (○) Halides; (□) phenolates; (△) acetates; (intersecting lines in left corner) bR_{568}.

The general properties of the PSB hydrogen bond may be summarized as follows [see, e.g., Hofacher (1983)]: (i) the *stronger* the hydrogen bond, the shorter the distance between the nitrogen and the counterion and the longer the N–H bond; (ii) with increasing hydrogen bond strength, the N–H bond becomes more polar; (iii) there will be minor electron charge transfer from the counterion to the nitrogen; (iv) the mutual polarization of the PSB and the counterion extends over several bonds; and (v) the orientation of the counterion and the PSB with respect to one another will be determined by attractive classical electrostatic and quantum-mechanical (exchange) interactions; the weaker the hydrogen bond, the more predominant the classical part of these interactions. In the following, we first describe the results obtained for the model compounds and their relationship to this scheme and then discuss the implications for bR.

PSB Model Compounds. The model compounds that we have studied can be divided into three classes, as shown in Table II. The halide salts show a strong upfield shift over the progression chloride–bromide–iodide. These results have been discussed previously and interpreted in terms of the strength of the nitrogen–counterion interaction (Harbison et al., 1983). From a crystallographic comparison of simple primary, secondary, and tertiary amines involving halide counterions, it is known that anions such as chloride hydrogen bond strongly to the conjugate acids of tertiary organic bases (Lindgren & Olovsson, 1968). The hydrogen bond is manifest primarily in the nitrogen–counterion distance; in particular, a hydrogen

Table II: ^{15}N Shift Tensor Elements σ_{11}, σ_{22}, and σ_{33} and Isotropic Shifts σ_i from MAS Experiments, Together with the Isotropic Shifts $(1/3)Tr(\sigma)$ As Obtained from Static Powder Pattern Measurements for the *N-all-trans*-Retinylidene Butylimine Salt Model Compounds[a]

	σ_{11}	σ_{22}	σ_{33}	σ_i	$(1/3)Tr(\sigma)$	pK_a[b]
halides						
iodide	26.3	163.8	273.8	154.5	154.6	−9.25
bromide	26.7	183.3	286.6	166.1	165.5	−8.5
chloride	27.3	194.6	296.3	171.7	172.5	−6.1
phenols						
2,4,6-trinitro	20.7	176.6	282.3	160.9	159.9	0.37
2-chloro-4,6-dinitro	19.8	184.2	291.9	165.3	165.3	2.1
2,4-dibromo-3,6-dinitro	20.1	187.7	292.8	168.4	166.9	2.9
2,6-dibromo-4-nitro	19.2	190.4	297.6	169.8	169.1	3.4
carboxylic acids						
trichloroacetic	24.4	165.2	276.6	154.2	155.4	0.51
trifluoroacetic	24.9	173.5	283.1	160.5	160.4	0.52
tribromoacetic	24.2	182.5	286.5	164.8	164.4	0.72
difluoroacetic[c]	22.5	194.2	298.2	173.6 169.7	171.6	1.34
dichloroacetic	22.5	204.7	295.2	174.7	174.1	1.35

[a] All shifts are given in ppm relative to external 5.6 M $^{15}NH_4Cl$ in H_2O. Estimated errors are 1 ppm for the principal values and 0.2 ppm for the isotropic shifts. For the discussion, the pK_a values of the conjugate acids are also listed. [b] Halide pK_a's from Perrin (1969). Organic pK_a's from Serjeant and Dempsey (1979), except for 2,4-dibromo-3,6-dinitrophenol, which was estimated by assuming that a 3-nitro group lowers the pK of 2,4-dibromo-6-nitrophenol (pK_a 4.7) by 1.8 pK units. This method works to an accuracy of ±0.3 pK unit for six other brominated and nitrated phenols tested. [c] The spectrum for the difluoroacetic acid salt showed two components, probably due to different crystallographic forms.

bond only exists if this distance is larger than the corresponding covalent bond distance, and smaller than the sum of the van der Waals radii of the respective ions. The upper limit discriminates the hydrogen bond from the ionic bond, where there is no penetration of atomic orbitals on the two ions. Decreasing distance below this limit is commonly used as the defining criterion for the strength of the hydrogen bond.

For the halides, the variation in N–H bond length associated with a change in hydrogen bond strength can be detected either directly by neutron diffraction or dipolar–chemical shift NMR spectroscopy (Roberts et al., 1987) or indirectly via its effect on vibrational frequencies, the proton chemical shift of the Schiff base proton, the deuterium quadrupole coupling constant of a Schiff base N–D (Berglund & Vaughan, 1981), and the ^{15}N chemical shift of the Schiff base nitrogen. A variation in nitrogen–counterion bond strength is expected to affect the nitrogen chemical shifts via one or both of two distinct mechanisms. First, the proximity of the counterion in a strongly hydrogen-bonded system will tend to increase the σ electron density on the nitrogen [see (ii) and (iii) above], causing *increased* shielding of that nucleus and a *decrease* in its chemical shift. This effect has been used to rationalize the chemical shifts of ammonium ions in the solid state (Ratcliffe et al., 1983). For example, ammonium chloride has a chemical shift 2 ppm higher than the corresponding bromide, and, because these two salts are isomorphous, the difference in chemical shift may be attributed to variation in hydrogen bonding. These results also suggest that the effects of counterion proximity are small. The second, more important mechanism results from the mutual polarizability of the Schiff base and the counterion [see (iv) above]. The conjugated retinal system is always easily polarized via the π electrons, whereas the polarizability of the halide ion increases with the radius on descending the sequence. In going from a larger to a smaller halide, stronger polarization of the conjugated system is expected because of the decrease in ion–counterion distance and the reduced polarizability of the counterion. This would cause a decreased π-electron density on the nitrogen and on the even-numbered carbons of the conjugated chain, and an increase in the electron density on the odd-numbered carbons (Kropf & Hubbard, 1958). The decreased charge density on the nitrogen will cause a *deshielding* of the nitrogen and an *increased* chemical shift, opposing the σ-electron effect.

That this π-electron effect may be expected to be rather large was demonstrated in a comparison of the carbon and nitrogen chemical shifts of the solid retinal Schiff base chloride and bromide, in which one observes an increased chemical shift for the nitrogen and the even-numbered carbons of the chloride salt and a decreased shift for the odd carbons (with the exception of the first carbon next to the nitrogen, which is anomalous in this respect), the effect tapering off as one proceeds down the chain (Harbison et al., 1985b). The regularity of the carbon chemical shift changes, and their dependence on proximity to the nitrogen is in agreement with the mutal polarization mechanism (iv) and lends credence to the supposition that we are observing local changes in bonding at the nitrogen in these model compounds.

While structures of the phenolate and carboxylate salts of organic bases have not been studied as systematically as the halide salts, we can nonetheless make inferences about their hydrogen-bonding ability from the pK_a of the anions' parent acids (see Table II). For the halides, there appears to be a correlation between NMR chemical shifts and the measured apparent pK_a in aqueous solution (Perrin, 1969). A similar strong correlation is noted for the phenolate series, where again low anion pK_a is associated with low chemical shifts, and vice versa. Finally, while the trend is not so obvious for the carboxylate salts—because of the smaller range of accessible pK_a's—nonetheless, it is clear that the three isotropic chemical shifts observed for the two higher pK_a dihaloacetates are higher than those of the three trihaloacetates.

The low pK_a of trinitrophenol and similar strong organic acids is thought to be due to the fact that the anions are stabilized by delocalization of the negative charge over all of the electronegative groups of the molecule. This gives rise to a reduction in the negative charge on the phenolic oxygen directly involved in hydrogen bonding to the cation, which increases with the number and strength of the electronegative substituents. One might therefore expect that these stronger acids will generate conjugate anions which hydrogen bond more weakly and will give rise to an increased charge density on the nitrogen. This inference is supported in our data by the nitrogen chemical shifts of the phenolate salts. Although it does not appear to affect the pK_a's as strongly, the same argument may be applied to explain the hydrogen-bonding properties of the carboxylate salts. Thus, it appears that within each class of counterions the ^{15}N chemical shifts correlate with the expected variation in hydrogen-bonding strength. The remaining question concerns comparisons between different classes.

Inspection of Figure 3 shows that polarization of the Schiff base nitrogen proceeds in essentially the same way for different counterions and bR_{568}. This indicates that the mechanism should be essentially independent of the detailed character of the counterion, while the *extent* of the process should reflect an effective overall strength of the counterion. Therefore, within the present context of NMR studies of protonated Schiff bases, it appears reasonable to define a "counterion strength" in terms of the measured chemical shift (i.e., the weaker the counterion, the lower the value of the chemical shift).

An interesting result that evolves from this definition is the absence of a universal correlation between the counterion strength and the pK_a of the conjugate acid in water. As an example, we consider the three counterions chloride, difluoroacetate, and 2,6-dibromo-4-nitrophenolate. Although their conjugate acids have widely different pK_a values (−6.1, 1.3, and 3.4, respectively), they have the same counterion strength, as measured by the ^{15}N NMR chemical shift (cf. Table II). Obviously, the mechanism for the stabilization of the anions in aqueous solution, through a hydrated complex, is substantially different from that in the solid, through crystal-field effects. Therefore, it is not sufficient to interpret interactions in proteins in terms of the solution pK_a values of the groups that are involved. In particular, it cannot be excluded that tyrosinates provide counterions and hydrogen bonds of comparable strength to aspartates and glutamates, despite their different pK_a values.

Bacteriorhodopsin. Only the bR_{568} results are strictly comparable to the model compound data, since we were able to prepare only all-trans protonated Schiff base salts. Table I shows that the σ_{11} element is very close to those of the model compounds, while σ_{22} and σ_{33} obey the same correlation observed for these compounds but show values which are even lower than those of the iodide salt. This suggests that bR_{568} has the properties of a normal, but very weakly hydrogen-bonded protonated Schiff base. Examination of the ^{13}C shifts of bR_{568} for the Schiff base end of the chromophore shows that they follow the same trend exhibited by the bromide model compound vis-ã-vis the chloride; that is, the perturbation in

chemical shift is largest at the nitrogen and falls off toward the middle of the chromophore (Harbison et al., 1985a). This again indicates that the perturbation at the nitrogen is a local polarization effect associated with a change in the (hydrogen) bonding of the Schiff base. It is unlikely that such behavior would result from an electrostatic perturbation elsewhere on the chromophore. [The presumed electrostatic perturbation we observed at C_5 is similarly local in its effects (Harbison et al., 1985a).] Moreover, it is very unlikely that effects elsewhere in the conjugated system would result in the same behavior for σ_{22} and σ_{33} as those associated with the Schiff base counterion. For example, a comparison of *all-trans*,15-*anti*-bR_{568} with 13-*cis*,15-*syn* bR_{548} (cf. Table I) shows that σ_{11} and σ_{33} are essentially unperturbed and only σ_{22} changes. This behavior is paralleled by the three carbons immediately adjacent to the Schiff base linkage, which also exhibit large effects in σ_{22} (Smith et al., 1989).

The model compound data seem to exclude direct interaction of the Schiff base with either a single carboxyl group (Fischer & Oesterhelt, 1979; Herz et al., 1983; Eisenstein et al., 1987; Roepe et al., 1987) or a single tyrosinate residue (Rothschild et al., 1986; Dollinger et al., 1986; Roepe et al., 1987). In order to produce chemical shifts in the acetate PSB model compounds in the neighborhood of 154 ppm and in the phenolate PSB model compounds as low as 161 ppm, it was necessary to attach multiple electronegative substituents, such as fluoro, chloro, bromo, and nitro groups. Even then, the chemical shift in bR_{568} is an additional 11 ppm lower than that for the most favorable model compound in this series, the trichloroacetate salt.

How can we account for such a weak interaction in a chemically satisfactory manner? While it is possible that the protein holds the counterion rigidly at a relatively large distance from the Schiff base, such a model is inconsistent with our knowledge of the general mobility and flexibility of the interior of proteins, as well as conflicting with the general properties of the hydrogen bond [see (v)]. We therefore propose that the counterion, rather than being a "naked" phenolate or carboxylate, is a complex ion in which several neutral protic species, such as water molecules and serine, tyrosine, or aspartate hydroxyls, may take part. Water-mediated salt bridges between protonated nitrogen bases and carboxylate anions have been detected in papain (Berendson, 1975) and carboxypeptidase A (Hartsuck & Lipscomb, 1971). It is anticipated that such complex ions may give rise to much weaker hydrogen bonds than individual ionic species.

Both cationic and anionic complex ions derived from oxygen bases have been described in the crystallographic literature. When the nitrogen–ligand distance is used as a criterion of bond strength, certain complex ions tend to contain much weaker bonds than comparable simple ionic substances. An example occurs in the series of compounds NH_4NO_3, $NH_4NO_3 \cdot HNO_3$, and $NH_4NO_3 \cdot 2HNO_3$. In the various phases of simple ammonium nitrate, nitrogen–oxygen distances are in the range 2.75–2.95 Å (Wyckoff, 1964a), well inside the range for hydrogen bonding (<3.0 Å for the N–H–O bond). At the other end of the series, in $NH_4NO_3 \cdot 2HNO_3$, the closest ammonium nitrogen–nitric acid oxygen distances are between 3.02 and 3.11 Å (Einstein & Tuck, 1970), more in the range for ionic bonding. The anion is the hydrogen-bonded complex $[O_2NO{-}H{-}(NO_3){-}H{-}ONO_2]^-$. Three nitrate anions combined with two protons forming two strong intraionic hydrogen bonds create a highly stable anion, leaving the third proton almost completely free for an ionic bond with the ammonium. A similar process takes place in the intermediate compound in the series, where two nitrate ions are stabilized by one proton in a strong intraionic hydrogen bond to form the $[O_2NO{-}H{-}ONO_2]^-$ complex (Duke & Llewellyn, 1950). Another example, involving a complex cation, occurs in $NH_4I \cdot 4NH_3$. In this case, the nitrogen–iodine distances are 3.96–4.16 Å (Olovsson, 1960), in the range of an ionic bond, as opposed to 3.62–3.78 Å for the various phases of ammonium iodide (Wyckoff, 1964b), which are in the hydrogen-bond range (<3.9 Å for N–H–I bonds). This complex cation contains four ammonia molecules linked through hydrogen bonds, with one excess proton.

In addition to explaining the spectroscopic data, a complex anion in bR has several other attractive features. First, it provides a role for tightly bound water molecules at the protein active site: this tightly bound water has been detected in vibrational studies (Hildebrandt & Stockburger, 1984) and may be involved in the comparatively rapid exchange of the Schiff base proton with bulk water (Harbison et al., 1988). It is also notable that removal of the tightly bound water molecule causes a substantial blue shift in the chromophore absorption maximum (Hildebrandt & Stockburger, 1984). Second, a complex ion also provides connectivity between the Schiff base and proton-conducting pathways operative in the bR photocycle. Third, a weakly hydrogen-bonded chromophore with a complex counterion is in accord with vibrational and optical characteristics of the chromophore which, like the NMR spectroscopic parameters, are beyond the extremes of the range of available model compounds. Fourth, a complex counterion may explain why the counterion has not been identified in single-site mutagenesis studies (Mogi et al., 1987, 1988; Hackett et al., 1987): If the counterion is sufficiently complex, removal of only one of the protic groups may have little effect on the overall counterion properties. Finally, the model places the bR chromophore in a different context and should provide impetus for further experimental work designed at better understanding the Schiff base environment in bR.

Conclusions

In the present work, we have shown that there exist remarkable similarities in the mechanism which governs the nitrogen chemical shift effects in bR and PSB model compounds. It is also clear that studying protonation effects in the solid state provides a more complete picture of the factors determining chemical shifts than is obtained from solution studies (Witanowski et al., 1981). High-resolution solid-state NMR, in combination with low temperatures in order to improve the signal-to-noise ratio, provides the necessary means to execute such investigations in membrane proteins like bR. The ^{15}N NMR data for bR strongly suggest that the counterion of the Schiff base is extremely weak. Furthermore, comparison with the PSB model compounds indicates that a direct interaction with a single ionized amino acid residue may not suffice to produce the observed hydrogen bond effects, and that a more complex counterion involving multiple species may be present.

Acknowledgments

We thank K. W. Fishbein, D. P. Raleigh, and S. O. Smith for their assistance with various phases of these experiments and for critically reading the manuscript.

Registry No. *N-all-trans*-Retinylidene butylimine iodide, 65727-80-2; *N-all-trans*-retinylidene butylimine bromide, 90550-44-0; *N-all-trans*-retinylidene butylimine chloride, 61769-46-8; *N-all-trans*-retinylidene butylimine 2,4,6-trinitrophenol, 118248-99-0; *N-all-trans*-retinylidene butylimine 2-chloro-4,6-dinitrophenol, 118249-00-6; *N-all-trans*-retinylidene butylimine 2,4-dibromo-3,6-dinitrophenol,

118249-02-8; *N-all-trans*-retinylidene butylimine 2,6-dibromo-4-nitrophenol, 118249-03-9; *N-all-trans*-retinylidene butylimine trichloroacetate, 118249-04-0; *N-all-trans*-retinylidene butylimine trifluoroacetate, 80704-07-0; *N-all-trans*-retinylidene butylimine tribromoacetate, 118249-05-1; *N-all-trans*-retinylidene butylimine difluoroacetate, 118249-06-2; *N-all-trans*-retinylidene butylimine dichloroacetate, 90550-45-1.

REFERENCES

Andrew, E. A., Bradbury, A., & Eades, R. G. (1958) *Nature (London) 182*, 1659.

Argade, P. V., Rothschild, R. J., Kawamoto, A. H., Herzfeld, J., & Herlihy, W. C. (1981) *Proc. Natl. Acad. Sci. U.S.A. 78*, 1643–1646.

Aton, B., Doukas, A. G., Callender, R. M., Becher, B., & Ebrey, T. G. (1977) *Biochemistry 16*, 2995–2999.

Bagley, K., Collinger, G., Eisenstein, L., Singh, A. K., & Zimanyi, L. (1982) *Proc. Natl. Acad. Sci. U.S.A. 79*, 4972–4976.

Berendson, H. J. C. (1975) in *Water: a Comprehensive Treatise* (Franks, F., Ed.) pp 293–330, Plenum Press, New York.

Berglund, B., & Vaughan, R. W. (1981) *J. Chem. Phys. 27*, 2037–2043.

Blatz, P., & Mohler, J. (1975) *Biochemistry 14*, 2304–2309.

Childs, R. F., Shaw, G. S., & Wasylishen, R. E. (1987) *J. Am. Chem. Soc. 109*, 5362–5366.

De Groot, H. J. M., Copiē, V., Smith, S. O., Allen, P. J., Winkel, C., Lugtenburg, J., Herzfeld, J., & Griffin, R. G. (1988) *J. Magn. Reson. 77*, 251–257.

Dollinger, G., Eisenstein, L., Lin, S.-L., Nakanishi, K., & Termini, J. (1986) *Biochemistry 25*, 6524–6533.

Doukas, A., Pande, A., Suzuki, R., Callender, R. H., Honig, B., & Ottolenghi, M. (1981) *Biophys. J. 33*, 275–280.

Druckmann, S., Ottolenghi, M., Pande, J., & Callender, R. H. (1982) *Biochemistry 21*, 4953–4959.

Duke, J. R. C., & Llewellyn, F. J. (1950) *Acta Crystallogr. 3*, 305–309.

Ehrenberg, B., Lewis, A., Porta, T. K., Nagle, J. F., & Stoeckenius, W. (1980) *Proc. Natl. Acad. Sci. U.S.A. 77*, 6571–6573.

Einstein, F. N. B., & Tuck, D. G. (1970) *Acta Crystallogr. B26*, 1117–1120.

Eisenstein, L., Lin, S.-L., Dollinger, G., Odashima, K., Termini, J., Konno, K., Ding, W.-D., & Nakanishi, K. (1987) *J. Am. Chem. Soc. 109*, 6860–6862.

Favrot, J., Sandorfy, C., & Vocelle, D. (1978) *Photochem. Photobiol. 28*, 271–272.

Fischer, U. C., & Oesterhelt, D. (1979) *Biophys. J. 28*, 211–230.

Gochnauer, M. B., & Kushner, D. J. (1969) *Can. J. Microbiol. 15*, 1157–1165.

Griffin, R. G., Aue, W. P., Haberkorn, R. A., Harbison, G. S., Herzfeld, J., Menger, E. M., Munowitz, M. G., Olejniczak, E. T., Raleigh, D. P., Roberts, J. E., Ruben, D. J., Schmidt, A., Smith, S. O., & Vega, S. (1988) in *Magic Angle Sample Spinning*, Proceedings of the International School of Physics "Enrico Fermi", Physics of NMR Spectroscopy in Biology and Medicine, July 8–18, 1986, Varenna, Italy, and North-Holland, Amsterdam.

Hackett, N. R., Stern, L. J., Chao, B. H., Kronin, K. A., & Khorana, H. G. (1987) *J. Biol. Chem. 19*, 9277–9284.

Harbison, G. S., Herzfeld, J., & Griffin, R. G. (1983) *Biochemistry 22*, 1–5.

Harbison, G. S., Smith, S. O., Pardoen, J. A., Courtin, J. M. L., Lugtenburg, J., Herzfeld, J., Mathies, R. A., & Griffin, R. G. (1985a) *Biochemistry 24*, 6955–6962.

Harbison, G. S., Mulder, P. P. J., Pardoen, H., Lugtenburg, J., Herzfeld, J., & Griffin, R. G. (1985b) *J. Am. Chem. Soc. 107*, 4809–4816.

Harbison, G. S., Roberts, J. E., Herzfeld, J., & Griffin, R. G. (1988) *J. Am. Chem. Soc. 110*, 7221–7223.

Hartsuck, J. A., & Lipscomb, W. N. (1971) *Enzymes (3rd Ed.) 3*, 1–56.

Henderson, R., & Unwin, P. (1975) *Nature 257*, 28.

Herz, J. M., Hrabeta, E., & Packer, L. (1983) *Biochem. Biophys. Res. Commun. 114*, 872–881.

Herzfeld, J., & Berger, A. E. (1980) *J. Chem. Phys. 73*, 6021–6030.

Heyde, M. E., Gill, D., Kilponen, R. G., & Rimai, L. (1971) *J. Am. Chem. Soc. 93*, 6776–6780.

Hildebrandt, P., & Stockburger, M. (1984) *Biochemistry 23*, 5539–5548.

Hodgson, H. H., & Smith, E. W. (1931) *J. Chem. Soc.*, 2269–2272.

Hofacher, G. L. (1983) in *Biophysics* (Hoppe, W., Lohmann, W., Murkl, H., & Ziegler, H., Eds.) Springer, Berlin.

Holleman, M. A. (1902) *Recl. Trav. Chim. Pays-Bas*, 432–440.

Honig, B., Greenberg, A. D., Dinur, U., & Ebrey, T. G. (1976) *Biochemistry 15*, 4593–4599.

Khorana, H. G., Gerber, G. E., Herlihy, W. C., Gray, C. P., Anderegg, R. J., Nibei, K., & Biemann, K. (1979) *Proc. Natl. Acad. Sci. U.S.A. 76*, 5046–5050.

Kropf, A., & Hubbard, R. (1958) *Ann. N.Y. Acad. Sci. 74*, 266–280.

Lewis, A., Spoonhower, J., Bogomolni, R. H., Lozier, R. H., & Stoeckenius, W. (1974) *Proc. Natl. Acad. Sci. U.S.A. 71*, 4462–4465.

Lindgren, J., & Olovsson, I. (1968) *Acta Crystallogr. B24*, 554–558.

Linnemann, E., & Stersch, A. (1867) *Jahresber. Fortschr. Chem.*, 532–732.

Lugtenburg, J., Muradin-Szweykowska, M., Heeremans, C., Pardoen, J. A., Harbison, G. S., Herzfeld, J., Griffin, R. G., Smith, S. O., & Mathies, R. A. (1986) *J. Am. Chem. Soc. 108*, 3104–3105.

Maricq, M. M., & Waugh, J. S. (1979) *J. Chem. Phys. 70*, 3300–3316.

Mathies, R., Freedman, T., & Stryer, L. (1977) *J. Mol. Biol. 109*, 367–372.

Mehring, M., Weber, T., Muller, W., & Wegner, G. (1982) *Solid State Commun. 45*, 1079–1082.

Mogi, T., Stern, L. J., Hackett, N. R., & Khorana, H. G. (1987) *Proc. Natl. Acad. Sci. U.S.A. 84*, 5595–5599.

Mogi, T., Stern, L. J., Marti, T., Chao, B. H., & Khorana, H. G. (1988) *Proc. Natl. Acad. Sci. U.S.A.* (in press).

Nakanishi, K., Balogh-Nair, V., Arnaboldi, M., Tsujimoto, K., & Honig, B. (1980) *J. Am. Chem. Soc. 102*, 7945–7947.

Oesterhelt, D., & Stoeckenius, W. (1974) *Methods Enzymol. 31*, 667–678.

Olovsson, I. (1960) *Acta Chem. Scand. 14*, 1466–1474.

Ovchinnikov, Tu. A., Abdulaev, N. G., Fergina, M. Yu., Kiselev, A. V., & Lobanov, N. A. (1979) *FEBS Lett. 100*, 219–224.

Perrin, D. D. (1969) in *Dissociation constants of Inorganic Acids and Bases in Aqueous Solution*, Butterworths, London.

Pines, A., Gibby, M. G., & Waugh, J. S. (1973) *J. Chem. Phys. 59*, 569–575.

Ratcliffe, C. I., Ripmeester, J. A., & Tse, J. S. (1983) *Chem. Phys. Lett. 99*, 177–181.

Roberts, J. E., Harbison, G. S., Munowitz, M. G., Herzfeld, J., & Griffin, R. G. (1987) *J. Am. Chem. Soc. 109*, 4163–4169.
Rodman-Gilson, H. S., Honig, B. H., Croteau, A., Zarrilli, G., & Nakanishi, K. (1988) *Biophys. J. 53*, 261–269.
Roepe, P., Ahl, P. L., Das Gupta, S. K., Herzfeld, J., & Rothschild, K. J. (1987) *Biochemistry 26*, 6696–6707.
Rothschild, K. J., & Marrero, H. (1982) *Proc. Natl. Acad. Sci. U.S.A. 79*, 4045–4049.
Rothschild, K. J., Argade, P. V., Earnest, T. N., Huang, K.-S., London, E., Liao, M. J., Bagley, H., Khorana, H. G., & Herzfeld, J. (1982) *J. Biol. Chem. 257*, 8592–8595.
Rothschild, K. J., Roepe, P., Ahl, P. L., Earnest, T. N., Bogomolni, R. A., Das Gupta, S. K., Mulliken, C. M., & Herzfeld, J. (1986) *Proc. Natl. Acad. Sci. U.S.A. 83*, 347–351.
Sandorfy, C., Lussier, L. S., Thanh, H. L., & Vocelle, D. (1987) *Biophysical Studies of Retinal Proteins* (Debrey, T. G., Frauenfelder, Honig, H. B., & Nakanishi, K., Eds.) pp 247–251, University of Illinois Press, Urbana—Champaign, IL.
Serjeant, E. P., & Dempsey, B. (1979) in *Ionisation constants of Organic Acids in Aqueous Solution*, Pergamon, New York.
Sheves, M., & Nakanishi, K. (1983) *J. Am. Chem. Soc. 105*, 4033–4039.
Smith, S. O., Myers, A. B., Mathies, R. A., Pardoen, J. A., Winkel, C., van den Berg, E. M. M., & Lugtenburg, J. (1985) *Biophys. J. 47*, 653–664.
Smith, S. O., Harbison, G. S., Raleigh, D. P., Roberts, J. E., Pardoen, J. A., Das Gupta, S. K., Mulliken, C., Mathies, R. A., Lugtenburg, J., Herzfeld, J., & Griffin, R. G. (1986) in *Biomolecular Stereodynamics III*, Proceedings of the Fourth Convention in the Discipline Biomolecular Stereodynamics, State University of New York, Albany, NY, June 4–9, 1985 (Sarma, R. H., & Sarma, M. H., Eds.) Adenine Press, Guilderland, NY.
Smith, S. O., Braiman, M. S., Myers, A. B., Pardoen, J. A., Courtin, J. M. L., Winkel, C., Lugtenburg, J., & Mathies, R. A. (1987) *J. Am. Chem. Soc. 109*, 3108–3125.
Smith, S. O., de Groot, H. J. M., Gebhard, R., Courtin, J. M. L., Lugtenburg, J., Herzfeld, J., & Griffin, R. G. (1989) *Biochemistry* (submitted for publication).
Spudich, J. L., McCain, D. A., Nakanishi, K., Okabe, M., Shimizu, N., Rodman, H., Honig, B., & Bogomolni, R. A. (1986) *Biophys. J. 49*, 479–483.
Stoeckenius, W., & Bogomolni, R. A. (1982) *Annu. Rev. Biochem. 52*, 587–616.
Terao, T., Maeda, S., Yamabe, T., Akagi, K., & Shirakawa, H. (1984) *Chem. Phys. Lett. 103*, 347.
Witanowski, M., Stefaniak, L., & Webb, G. A. (1981) *Annu. Rep. NMR Spectrosc. 11B*, 33–34.
Wyckoff, R. W. G. (1964a) *Crystal Structures*, Vol. 1, pp 88, 104, Wiley, New York.
Wyckoff, R. W. G. (1964b) *Crystal Structures*, Vol. 2, pp 368–374, Wiley, New York.

A Continuous Assay for Lipases in Reverse Micelles Based on Fourier Transform Infrared Spectroscopy

Peter Walde and Pier Luigi Luisi*
Institut für Polymere, Eidgenössische Technische Hochschule, CH-8092 Zürich, Switzerland
Received July 14, 1988; Revised Manuscript Received November 30, 1988

ABSTRACT: A new, simple, and fast method is described for measuring the lipase-catalyzed hydrolysis of triglycerides in reverse micelles. The course of hydrolysis can be followed by recording the Fourier transform infrared spectrum of the entire reaction mixture as a function of incubation time. Due to the presence of isosbestic points, the kinetics of the reaction can be followed at different regions of the spectrum, for example, in the stretching band region of carbon–oxygen double or single bonds (between 1750 and 1710 cm^{-1} or around 1160 cm^{-1}, respectively). It is shown that the method can be applied for determining the extent of hydrolysis and for the determination of the lipolytic enzyme's fatty acid specificity within the class of triglycerides.

There is a growing interest in lipases not only for their applications in fat hydrolysis and synthesis under mild conditions (Linfield et al., 1984) but also for their use as catalyst for a variety of reactions, e.g., aminolysis, thiotransesterifications, and oximolysis. One of the problems in the enzymology of lipases is the lack of a simple spectrophotometric assay with triglyceride substrates. The reason lies in the poor water solubility of both synthetic and natural substrates.

The use of reverse micelles can in principle overcome these difficulties. In fact, one of the peculiarities of enzymes in reverse micelles (or "water-in-oil microemulsions" at higher water content) is their capability of being active with substrates that are present in the oil (organic solvent) phase [for reviews see Luisi (1985), Martinek et al. (1986), Waks (1986), and Luisi and Steinmann-Hofmann (1987)]. Generally, in a reverse micelle solution, the enzyme is solubilized within the aqueous core of the micelle and protected against unfavorable contacts with the organic solvent by a layer of surfactant molecules (Martinek et al., 1986; Luisi et al., 1988). In clear contrast to those cases where enzyme powders are directly dispersed in organic solvents without surfactants (Zaks & Klibanov, 1985), reverse micellar solutions are stable and optically transparent systems, allowing one to carry out spectroscopic studies. Several previous papers have considered phospholipases/lipases in reverse micelles (Misiorowski & Wells, 1974; Malakhova et al., 1983; Fletcher et al., 1985,

0006-2960/89/0428-3353$01.50/0